

Variability among polysulphone calibration curves

**G R Casale¹, M Borra², A Colosimo³, M Colucci², A Militello²,
A M Siani¹ and R Sisto²**

¹ University of Rome 'La Sapienza', Physics Department, P.le A. Moro 2, I-00185, Rome, Italy

² ISPESL, (Istituto Superiore per la Prevenzione E la Sicurezza del Lavoro), Occupational Hygiene Department, Via Fontana Candida 1, I-0040 Monteporzio Catone (RM), Italy

³ University of Rome 'La Sapienza', Department of Human Physiology and Pharmacology, P.le A. Moro 2, I-00185, Rome, Italy

E-mail: renata.sisto@ispesl.it

Received 7 June 2006, in final form 14 July 2006

Published 15 August 2006

Online at stacks.iop.org/PMB/51/4413

Abstract

Within an epidemiological study regarding the correlation between skin pathologies and personal ultraviolet (UV) exposure due to solar radiation, 14 field campaigns using polysulphone (PS) dosimeters were carried out at three different Italian sites (urban, semi-rural and rural) in every season of the year. A polysulphone calibration curve for each field experiment was obtained by measuring the ambient UV dose under almost clear sky conditions and the corresponding change in the PS film absorbance, prior and post exposure. Ambient UV doses were measured by well-calibrated broad-band radiometers and by electronic dosimeters. The dose-response relation was represented by the typical best fit to a third-degree polynomial and it was parameterized by a coefficient multiplying a cubic polynomial function. It was observed that the fit curves differed from each other in the coefficient only. It was assessed that the multiplying coefficient was affected by the solar UV spectrum at the Earth's surface whilst the polynomial factor depended on the photoinduced reaction of the polysulphone film. The mismatch between the polysulphone spectral curve and the CIE erythral action spectrum was responsible for the variability among polysulphone calibration curves. The variability of the coefficient was related to the total ozone amount and the solar zenith angle. A mathematical explanation of such a parameterization was also discussed.

1. Introduction

Following the discovery of the Antarctic ozone hole in 1985 and the significant decrease in total ozone at middle latitudes observed since the 1970s, solar ultraviolet (UV) radiation became an important environmental, ecological and atmospheric parameter to be measured and studied (Webb 1998, WMO 2002, van der Leun 2004). Increasing interest has been shown

by the scientific community in human health risks deriving from over-exposure to solar UV radiation. In fact, harmful effects include some kinds of skin cancer and some eye pathologies (de Gruijl 1999, Diffey 2004), whereas the only well-established beneficial effect of solar UV radiation is the production of vitamin D₃ required for skeleton health (Holick 2000).

According to the Commission Internationale de l'Eclairage, CIE, the UV region is subdivided into UVC (100–280 nm), UVB (280–315 nm) and UVA (315–400 nm). The amount of solar ultraviolet radiation reaching the Earth's surface depends on the amount of incoming solar energy, the transmission properties of the atmosphere and the properties of the surface (Webb 1998, Kerr 2003). No UVC radiation reaches the Earth's surface, since it is completely absorbed by ozone and molecular oxygen in the upper atmosphere.

Extensive UV monitoring by means of spectroradiometers and broad-band radiometers started during the 1990s (WMO 2002), although a homogeneous network for UV measurements does not yet exist (Kerr 2003, Seckmeyer 2000). Recently, UV measurements by multi-channel (moderate- and narrow-band) radiometers have also become available (Di Menno *et al* 2002, Bernhard *et al* 2003).

The degree of effectiveness of UV radiation in producing biological damage depends on the 'biologically effective solar exposure', or 'biologically effective dose', i.e. the incident weighted irradiance on a given surface over a specified period of time, expressed in joules per square metre, J m⁻² (Parisi 2005). The determination of the biologically effective dose requires knowledge of the action spectra of a biological system, i.e., of functions expressing the effectiveness of electromagnetic radiation in causing a specific response in that biological system. The erythral action spectrum is a weighting function that simulates the damage process occurring in the skin (Diffey and McKinlay 1987). However, although the biological action spectra can help in understanding some biological effects, they do not contain information on the simultaneous effect of multiple wavelengths and feedback mechanisms.

Values of the erythral ultraviolet irradiance between 280 and 400 nm, i.e. the dose rate, can be measured by broad-band instruments that have a spectral response matching the skin erythral response or, alternatively, calculated by using spectroradiometers and then weighting the irradiance with the CIE erythral action spectrum (CIE 1987). Both these instruments yield data of UV radiation incident upon a flat horizontal surface.

Dosimetry is widely used in epidemiological studies to quantify personal solar exposure of humans in different settings, during their ordinary daily activities. In fact, dosimetry enables measurements of the exposure of differently oriented surfaces and it can be used in remote and not easily accessible places (Webb 1995). Several erythral dosimeters have been developed: electronic solid state dosimeters (El Naggar *et al* 1995, Cockell *et al* 2001, Cockell *et al* 2002), dosimeters based on the metabolism of bacteria (Boldemann *et al* 2004, Quintern *et al* 1994) and dosimeters based on changes in the optical properties of specific materials following exposure to UV radiation (Davis *et al* 1976, Diffey and Davis 1978). This latter methodology involves the use of photosensitive films whose absorbance properties change upon exposure to UV radiation.

The most widely used photosensitive film is made by polysulphone (PS) polymer (Diffey 1989, Parisi *et al* 1997). This polymer undergoes photodegradation when exposed to UV radiation, leading to modification of its absorbance properties in the UV range. The spectral response of polysulphone (Diffey 1989) is similar to that of CIE erythral (figure 1). Absorbance at a given wavelength is measured before and after exposure and the observed difference depends on the erythral effective UV dose absorbed by the dosimeter (Diffey 1989). When this technique is used, it is recommended to determine the calibration curve in order to obtain reliable dose estimates (Diffey 1987, Kimlin 2003, Kollias *et al* 2003).

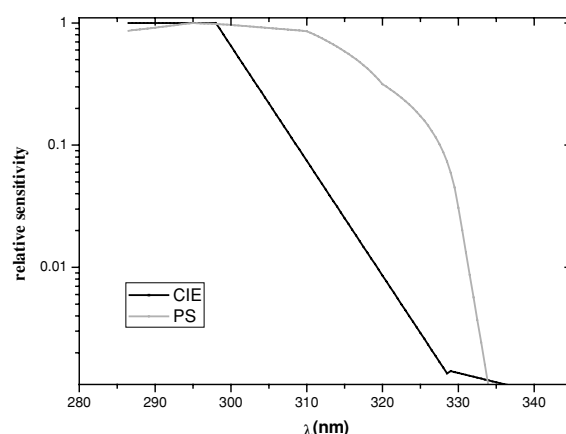


Figure 1. CIE and PS action spectra normalized at 295 nm.

In the present study the variability among the calibration curves obtained during 14 field experiments carried out in different environmental conditions (urban, rural and semi-rural sites) is analysed. Field campaigns were performed during 2004 and 2005 at three Italian sites between 41.9 °N and 43.3 °N, for solar zenith angle (SZA) ranging from about 20° to 70°. The observed variability among the calibration curves is here interpreted taking into account the site of the field experiment and important factors modulating the UV spectrum at the Earth's surface.

The purpose of this study is to combine the information deriving from the empirical relation between the erythema effective UV dose and the PS absorbance change with its mathematical explanation.

A parameterization of the calibration curves, represented by a coefficient multiplying a cubic polynomial function, is proposed. It is shown that the multiplying coefficient depends on the spectral shape of the UV radiation, which is mainly affected by the total ozone amount and the solar zenith angle, while the cubic polynomial function is assumed to be dependent on the PS photodegradation mechanisms only. This polynomial function, first proposed by Diffey (1987) on an empirical basis, is here explained in the appendix, based on the theoretical expressions for the PS response found by Krins *et al* (1999).

2. Materials and methods

2.1. Calibration curves of polysulphone films

Dosemeters are useful for determining UV doses absorbed by humans on different body parts, mainly when exposure conditions are characterized by high variability during outdoor activities (Parisi *et al* 1997, Kimlin *et al* 1998a). An exhaustive discussion about the properties and limitations of doseimeters was given by Webb (1995).

Polysulphone dosimetry is a widely tested methodology for assessing ultraviolet radiation exposure (Davis *et al* 1976, Diffey 1984, Kimlin *et al* 1998b). The use of PS doseimeters for a reliable quantification of personal doses requires the calibration curves to be determined. These curves are obtained by measuring the ambient erythema effective UV dose (hereafter called ambient UV dose) and the corresponding change in PS film absorbance (ΔA at 330 nm),

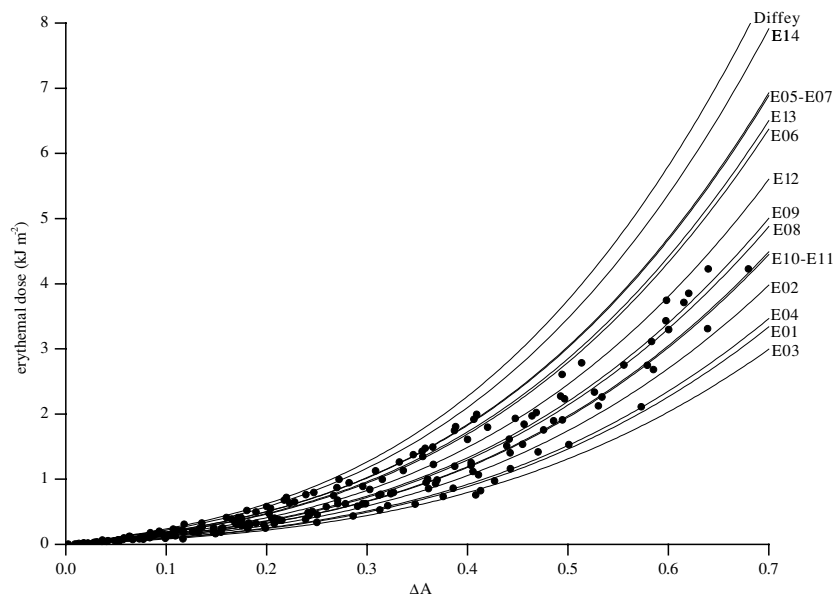


Figure 2. Calibration curves obtained in this study, and the Diffey cubic polynomial (the highest curve). Data points from calibrations are also reported (black dots).

prior and post exposure (Kimlin 2003). The absorbance of unexposed PS films with a thickness of 40 μm at 330 nm ranges from 0.1 to 0.2 depending on the batch, with increased values after the exposure to UV radiation. Under prolonged exposures the film reaches saturation at values of ΔA greater than about 0.4.

Diffey (1987) showed that the best data fit, mainly for $\Delta A > 0.3$, is given by the following equation:

$$D = c(\Delta A + \Delta A^2 + 9\Delta A^3), \quad (1)$$

where D (erythemal dose) is expressed in kJ m^{-2} . He found the value of the coefficient c equal to 2 kJ m^{-2} from a field campaign carried out on a summer day (1 July 1986) and on an autumn day (2 October 1986) at a site located at 55°N.

In this study, within an epidemiological study regarding the correlation between skin pathologies and personal ultraviolet exposure due to solar radiation, several field campaigns using polysulphone dosimeters were carried out at three Italian sites. A large variability was observed between the PS calibration curves (figure 2). The same variability can be observed also by comparing the Diffey curve to those of other studies (figure 3), such as the curve obtained in Antarctica in 2002 (ISS curve) during the summer season (Mariutti *et al* 2003) and those derived by Kimlin in the USA (K1, K2, K3 curves) and Australia (K4, K5 curves) (Kimlin, personal communication (2005)). The variability observed amounts to much more than 10%, which is the relative error associated with doses estimated by equation (1) (Diffey 1989), and it is clearly related to different ambient conditions. It is noteworthy that such a large variability cannot be attributed only to different thickness (all dosimeters are 40 μm thick) and batch.

In order to study this large variability among PS calibration curves in the local environmental conditions of middle-latitude sites, the following 14 field campaigns were carried out: six at an urban site (Rome, city centre); five at a semi-rural site (Monteporzio

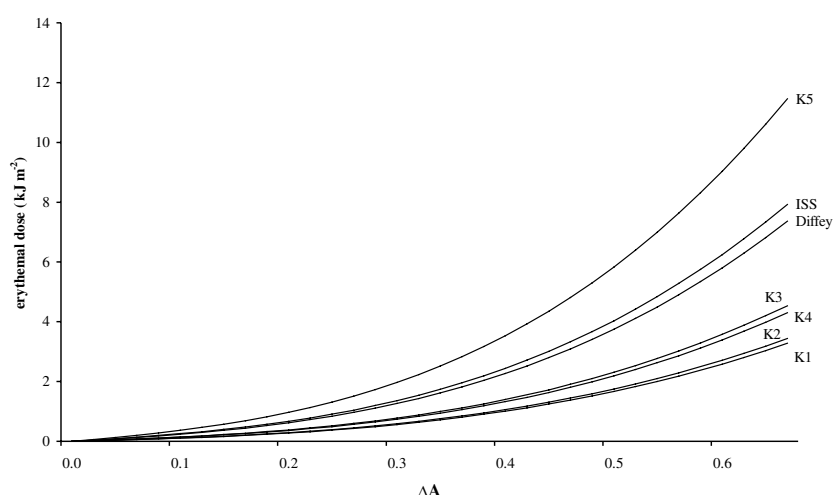


Figure 3. Comparison among different calibration curves: Diffey (1989), ISS (Mariutti *et al* 2003), K1, K2, K3, K4, K5 (Kimlin, personal communication (2005)).

Catone); three at a rural site (S Felice, Tuscany). All sites are located between 41.9 and 43.3 °N. Six campaigns were held during summer 2004 and 2005, two in winter 2004 and 2005, four in spring 2005 and two in autumn 2005. All field campaigns were conducted under almost completely clear sky conditions and for a solar zenith angle (SZA) in the range from 20° to 70°. The polysulphone film was mounted on a plastic holder with a central hole of about 1 cm² and three batches were used. Calibration curves were obtained using a number of dosimeters ranging from 10 to 20, located on a horizontal flat plane and exposed for different appropriate time intervals. Absorbance, before and after exposure to solar UV radiation, was measured in the laboratory either by a standard UV spectrophotometer (Perkin Elmer Lambda 5 UV-Vis double beam Spectrometer) or by a miniaturized and portable spectroradiometric system (Ocean Optics-Avantes AVS-SD 2000). In the latter case, a sample holder micrometry movement system moves the PS badge with high precision during irradiation by a xenon pulsed lamp and the absorbance was measured at the 330 nm emission peak of the source. More details on the spectroradiometer system can be found in Sisto *et al* (2001). The two reading methods were carefully compared using different film batches and no discrepancy was found in the change of optical absorbance at 330 nm.

2.2. Measurements of ambient UV doses

The use of dosimeters requires a calibration using well-calibrated solar UV instruments such as spectroradiometers or broad-band radiometers.

In this study ambient UV doses were measured by broad-band radiometers (model UVB-1, Yankee Environmental System, MA, USA) and by X2000-4 electronic dosimeters (Gigahertz-Optik, Puchheim, Germany). The YES radiometer has a spectral response similar to that of skin erythema and it measures the erythemal dose rate between 280 and 400 nm. The waveband is selected by means of the detector and of coloured glass filters. A phosphor filter converts incoming UVB radiation to green light, which is then measured by a solid-state photo-detector. The YES radiometer is equipped with an internal temperature control system for the phosphor

and related optical components. The system heats these components at a fixed temperature of 45 °C in the ambient temperature range between –40 °C and +40 °C. YES measurement is sampled at 1 min averages.

Two YES radiometers were used in this study. One belongs to the Solar Radiometry Observatory, University of Rome ‘La Sapienza’ (41.9 °N, 12.5 °E, 75 m asl). This radiometer (named here as the URO radiometer) is installed on the roof of a building on the University Campus (in the centre of Rome) and it has been working reliably since 2000. The Solar Radiometry Observatory is one of the stations that regularly measures UV irradiance in Italy, and it also has a Brewer spectrophotometer (operational since 1992) for measurements of UV spectral irradiance. Details can be found in Casale *et al* (2000). Ambient UV doses agree with those measured by the Brewer spectrophotometer at Rome ‘La Sapienza’, under clear sky conditions, with $\pm 10\%$ uncertainty (Siani *et al* 2003). The URO radiometer was calibrated at the European Reference Centre for Ultraviolet Radiation Measurements (Joint Research Centre, Ispra, Italy) in 2004.

The other YES radiometer (named here as the ISPESL radiometer) belongs to the ISPESL (Istituto Superiore per la Prevenzione E la Sicurezza sul Lavoro), Monteporzio Catone (41.8 °N, 12.7 °E, 300 m asl). This semi-rural site is about 30 km southeast of Rome. The performance of the ISPESL radiometer was tested during several field experiments using the URO radiometer as the reference instrument. The mean percentage difference between the two instruments during all field experiments was less than 5% showing their good agreement.

A complementary method for measuring ambient UV doses using X2000-4 electronic dosimeters was also used in this study. The X2000-4 electronic dosimeters are small and easy to use. They are powered by batteries during exposure and can be set up in not easily accessible areas. The electronic dosimeter is equipped with two photovoltaic cells, one reproducing the erythral action spectrum, the other having a response which is approximately constant in the UVA range (the UVB contribution is negligible). The instrument response is cosine corrected.

The acquisition sampling rate can be set using the dedicated software and, in this study, a frequency of 1 Hz was adopted. The absolute calibration of the electronic dosimeters was certified by Gigahertz-Optik in 2005.

3. Results

3.1. Calibration curves from different instruments

A comparison between the calibration curves obtained with broad-band radiometers and electronic dosimeters was carried out on 28 July 2005 in Rome under clear sky conditions. Ambient doses were calculated beginning with dose rates as 1 min averages of the irradiance values. Electronic dosimeters were exposed on a flat horizontal plane near the radiometer so that all instruments had the same field of view of 2π . Twenty PS dosimeters were used for differing time intervals starting at 7.00 UT.

Calibration curves obtained from the two different instruments are plotted in figure 4, showing a good agreement: the percentage difference $(X2000 - YES)/YES$ is -9% .

This result supports the use of electronic dosimeters to obtain calibration curves during field campaigns of personal solar exposure in sites where it is not possible to install radiometers. In this case it is however recommended to assess the agreement between the calibration curves of a well-calibrated standard UV instrument and electronic dosimeters.

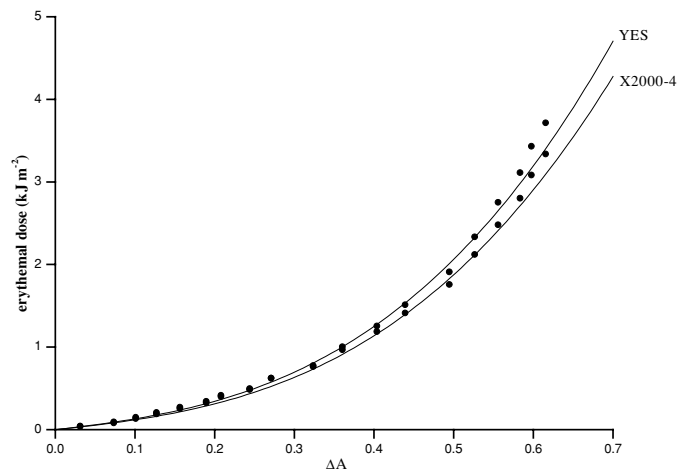


Figure 4. PS calibration curves on 28 July 2005 obtained using URO YES radiometer data and the average of the two GigaHertz Optic X2000–4 electronic dosimeters. The calibration equations are, respectively, $D = 1.1(\Delta A + \Delta A^2 + 9\Delta A^3)$ for the YES and $D = 1.0(\Delta A + \Delta A^2 + 9\Delta A^3)$ for the electronic devices. Data points from calibration are also reported (black dots).

Table 1. List of 14 calibration curves and the corresponding value of c (with the associated standard error). R is a measure of the goodness of the polynomial fit. Rome, Monteporzio and S Felice are respectively urban, semi-rural and rural sites.

	Date (dd/mm/yyyy)	Site	c (kJ m ⁻²)	R
E01	22/07/2004	Rome	0.78 ± 0.03	0.98
E02	13/12/2004	Rome	0.93 ± 0.01	0.99
E03	04/02/2005	Rome	0.70 ± 0.02	0.99
E04	09/03/2005	Monteporzio	0.81 ± 0.03	0.99
E05	21/03/2005	Monteporzio	1.61 ± 0.05	0.99
E06	06/04/2005	Monteporzio	1.49 ± 0.04	0.99
E07	22/04/2005	S Felice	1.62 ± 0.03	0.99
E08	21/06/2005	Rome	1.14 ± 0.02	0.99
E09	12/07/2005	S Felice	1.17 ± 0.03	0.99
E10	20/07/2005	Rome	1.04 ± 0.02	0.99
E11	28/07/2005	Rome	1.05 ± 0.01	0.99
E12	15/09/2005	Monteporzio	1.31 ± 0.03	0.99
E13	12/10/2005	S Felice	1.52 ± 0.04	0.99
E14	04/11/2005	Monteporzio	1.85 ± 0.04	0.99

3.2. Calibration curves from the field campaigns

The PS calibration curve for each of the 14 field campaigns was obtained by measuring ambient UV doses by means of YES radiometers or electronic dosimeters. Collected data for each campaign were best fitted using a cubic polynomial function with the same form of equation (1) but different values of the c coefficient. The dates and sites of the field experiments are listed in chronological order in table 1, while the calibration curves are plotted in figure 2 together with the Diffey curve. Values of c from the best fit procedure and its goodness (R) are also reported in table 1.

From figure 2 it can be seen that the calibration curves show a large variability, which is reflected in the values of the coefficient c , varying within a factor of more than 2. This effect cannot be due to differences among the PS dosimeters. Urban calibration curves have the smallest c values (average $0.94 \pm 0.02 \text{ kJ m}^{-2}$), which increase in the semi-rural and rural sites (average $1.41 \pm 0.04 \text{ kJ m}^{-2}$ and $1.44 \pm 0.03 \text{ kJ m}^{-2}$, respectively). Moreover, table 1 shows that there is variability among the calibration curves even within the same month.

4. Analysis of results and discussion

A mathematical interpretation of equation (1) is given in the appendix using a perturbative method, but it should be reminded that a complete justification of the coefficients in brackets is empirical.

Data collected from the field experiments indicate that the variability of the c coefficient could be attributed to the different environmental conditions during each field campaign. Keeping in mind that the polysulphone and the erythema have different responses beyond 300 nm (figure 1), special attention was focused on the total ozone amounts and solar zenith angle ranges. In order to investigate their effect on the calibration patterns, the STAR radiative transfer model (Ruggaber 1994) was used under clear sky conditions in an urban, a semi-rural and a rural scenario. The agreement between the UV measurements and the modelled values was already assessed in a field campaign in Rome (Meloni *et al* 2000). Here the model was used to calculate spectral irradiances from 280 to 400 nm with 0.5 nm wavelength steps, total ozone values O_3 ranging from 200 to 500 DU in steps of 50 DU and SZA ranging from 20 to 70° in steps of 10°. The sites were differentiated taking into account surface albedo, boundary layer height and tropospheric aerosol type, while the same standard values of stratospheric aerosol and vertical profiles of ozone, temperature and humidity, named US profiles were used. Modelled spectral irradiances were then convolved with the CIE erythema action spectrum and the PS action spectrum, and integrated over the entire wavelength range.

According to Krins *et al* (2001), the g factor was determined as follows:

$$g = \frac{\int I(\lambda) S_{\text{ery}}(\lambda) d\lambda}{\int I(\lambda) S_{\text{PS}}(\lambda) d\lambda}, \quad (2)$$

where $I(\lambda)$ is the solar spectral irradiance at the Earth's surface, $S_{\text{ery}}(\lambda)$ the CIE erythema action spectrum and $S_{\text{PS}}(\lambda)$ the polysulphone action spectrum. In the appendix we show that c can be expressed by dividing g by the constant $\alpha = 7.4 \times 10^{-5} \text{ m}^2 \text{ J}^{-1}$. The behaviour of g follows the variability of $I(\lambda)$, which is affected by atmospheric and geometric parameters.

The model was used to find out which factors play a major role in the fluctuation of g . No significant discrepancies were found in g values owing to the characterization of the site in terms of typical aerosol loading and surface albedo.

The analysis showed that total ozone and SZA are the main parameters affecting the variability of g . Values of g as a function of O_3 amounts and SZA, summarized in table 2, show that significant variations of g are related to lower O_3 and SZA values, while at higher O_3 and SZA levels no changes occur. This indicates that g variability is mainly modulated by changes of solar UVB irradiance where the erythema action spectrum is more effective. This is in agreement with the results shown by Krins *et al* (2001).

The values in table 2 allow us to estimate c (see table 3). In order to interpret the results, it is useful to distinguish two regions in table 3:

- the first region (dark grey) highlights that for $O_3 \leq 300 \text{ DU}$ and $\text{SZA} \leq 40^\circ$ the c values show a great variability (from 1.06 to 1.56 kJ m^{-2});

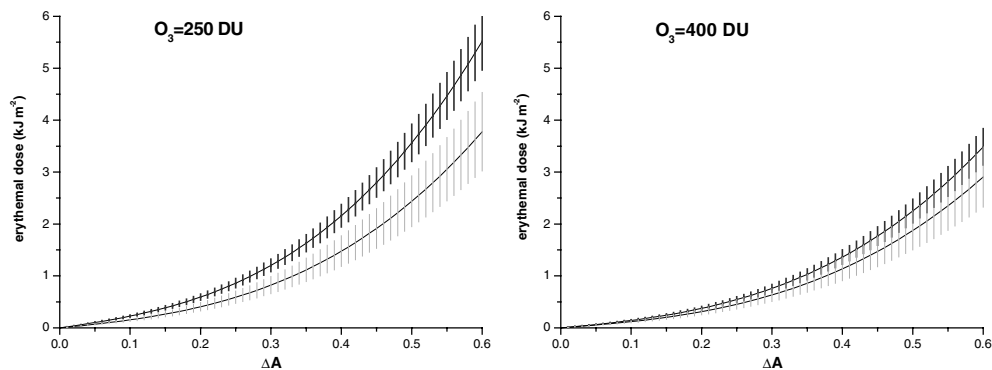


Figure 5. Measured (black) and modelled (grey) calibration curves for two different groups (left: $O_3 = 250$ DU, $SZA > 50^\circ$; right: $O_3 = 400$ DU, $SZA < 50^\circ$). The error bars are drawn as described in the text.

Table 2. Values of g as a function of total ozone (first column on the left, values in DU) and SZA (upper row, in degrees).

O_3/SZA	20	30	40	50	60	70
500	0.07	0.06	0.06	0.06	0.06	0.06
450	0.07	0.07	0.06	0.06	0.06	0.06
400	0.07	0.07	0.07	0.06	0.06	0.06
350	0.08	0.08	0.07	0.07	0.06	0.06
300	0.09	0.08	0.08	0.07	0.06	0.06
250	0.10	0.09	0.09	0.08	0.07	0.06
200	0.12	0.11	0.10	0.09	0.08	0.07

Table 3. Modelled values of c as a function of total O_3 (first column on the left, values in DU) and SZA (upper row, in degrees).

O_3/SZA	20	30	40	50	60	70
500	0.90	0.87	0.83	0.79	0.76	0.76
450	0.95	0.91	0.87	0.82	0.77	0.75
400	1.01	0.97	0.91	0.85	0.79	0.75
350	1.09	1.04	0.97	0.90	0.82	0.78
300	1.20	1.14	1.06	0.97	0.87	0.77
250	1.35	1.28	1.18	1.07	0.95	0.83
200	1.56	1.48	1.36	1.22	1.06	0.91

- the second (light grey) refers to $O_3 \geq 400$ DU and $SZA \geq 50^\circ$, where the c values are on average stable around 0.8 kJ m^{-2} .

A comparison between modelled (table 3) and measured (table 1) c values was performed taking into account four groups of total O_3 amounts (from 250 to 400 DU at 50 DU steps). Calibration curves, representative of each group, were then determined using the mean modelled and measured value of c in equation (1). The results for two different total ozone amounts (250 and 400 DU), representative of middle-latitude sites, are plotted in figure 5. The error bar assigned to each data point in figure 5 is 10% for the measured c and 20% for the modelled c (Schwander *et al* 1997). A comparison indicates that the calibration curves are

consistent for $O_3 = 400$ DU (measured $c = 1.22$, modelled $c = 0.96$) where the percentage difference, (measured – modelled)/measured, is 21%. In the case of $O_3 = 250$ DU (measured $c = 1.45$, modelled $c = 0.95$) the percentage difference is 34%.

The calibration curve is best fitted by a cubic expression with a multiplying coefficient c which is a function of g (see equation (2)). A mathematical interpretation is presented in the appendix, showing that the curve was obtained expanding the polysulphone response function to the limit of small doses and inverting the relation between the absorbance variation and the absorbed dose. It can be assessed that the multiplying coefficient is affected by the solar UV spectrum at the Earth's surface whilst the expression in brackets depends on the photoinduced reaction of polysulphone film dosimeters (Rivaton and Gardette 1999).

The mismatch between the polysulphone spectral curve and the CIE erythral action spectrum is responsible for the variability among polysulphone calibration curves. Since the erythemally weighed irradiance is much more sensitive to the UVB radiation than the irradiance weighted by the polysulphone response function, c follows total ozone fluctuations and solar zenith angle changes. Similar results were shown by Krins *et al* (2001).

The solar zenith angle is involved in the radiation absorption law:

$$I(SZA) = I(0) e^{-\alpha/\cos(SZA)}, \quad (3)$$

where $I(SZA)$ is the direct beam radiation at a fixed wavelength reaching the Earth's surface at SZA, $I(0)$ is the irradiance at the top of the atmosphere and α is the atmospheric extinction coefficient.

For small angles, the following equation is obtained:

$$I(SZA) = I(0) \left[1 - \alpha \left(1 - \frac{1}{2} SZA^2 + \dots \right) \right]. \quad (4)$$

Equation (4) yields that, for sufficiently small values of SZA, the dependence on the solar zenith angle is a second-order polynomial law. For increasing values of total ozone amount, the SZA dependence becomes negligible.

A best fitting procedure to describe the measured g values as functions of O_3 and SZA was performed by using the following relationship:

$$g(O_3, SZA) = g(200, 20) - aO_3 + bSZA - \hat{b}(SZA)^2 \quad (5)$$

where $g(200,20)$ is the g value at $O_3 = 200$ DU and $SZA = 20^\circ$.

If $g(200,20) = 0.12$, the best fit ($R^2 = 0.93$) to the measured values of g , according to equation (5), gives

$$\begin{aligned} a &= (1.3 \pm 0.2) \times 10^{-4} \text{ DU}^{-1} \\ b &= (7.8 \pm 1.5) \times 10^{-4} \text{ deg}^{-1} \\ \hat{b} &= (1.8 \pm 0.4) \times 10^{-5} \text{ deg}^{-2}. \end{aligned}$$

5. Conclusions

The quantification of human UV exposure is a complex issue. A methodology for recording the level of exposure for different body postures is based on the use of polysulphone, a polymer which changes its optical properties (absorbance) when exposed to UV radiation. Any polysulphone dosimetry measurement programme requires specific procedures, in particular the determination of the calibration curve (ambient dose versus absorbance difference at 330 nm, ΔA). The calibration curve is best fitted by a cubic polynomial function having a multiplying coefficient c that is proportional to the ratio g between the erythemally weighted irradiance and the PS weighted irradiance.

The aim of the present work was to analyse the polysulphone dosimeter calibration curves obtained during 14 field campaigns carried out at three different middle latitude sites (urban, semi-rural and rural sites) and in any season of the year. Curves were obtained by measuring ambient UV doses both with broad-band radiometers and electronic dosimeters. No significant discrepancies were observed using two different UV detectors in the determination of the calibration curve (percentage difference is 9%). The observed variability among the 14 calibration curves was interpreted through a critical study of the c coefficient. It was noted that the c values ranged from 0.78 to 1.85 kJ m⁻². Calibration curves were characterized in urban sites by the smallest c values (average 0.94 kJ m⁻²), which increase in the semi-rural and rural sites (average 1.41 and 1.44 kJ m⁻², respectively). Calibration curves change even if they are obtained in relatively short time periods within the same month. It was shown that such variability cannot be attributed to the different batch of the PS film since no significant discrepancies in ΔA at 330 nm were found.

In order to understand the factors affecting the calibration curve, a radiative transfer model was used, having as input the total ozone amount (from 200 to 500 DU) and the SZA (from 20 to 70°). It was found that when $O_3 \leq 300$ DU and $SZA \leq 40^\circ$ the modelled c coefficient showed a rather large variability (from 1.06 to 1.56 kJ m⁻²), while for $O_3 \geq 400$ DU and $SZA \geq 50^\circ$ the values of c were approximately stable, around 0.8 kJ m⁻². A theoretical interpretation of the variability of the calibration curves was also provided, showing that the c coefficient depended linearly on the total ozone amount while it followed a quadratic law in the solar zenith angle.

In conclusion, in personal UV measurement programmes, a careful quantification of the polysulphone calibration curve is recommended under the same atmospheric conditions of exposure of population groups. This implies that in the PS measurement programme a proper number of dosimeters should be planned for the characterization of the most reliable dose-response curve *in situ* and not in a laboratory environment by means of artificial sources. Future investigations will aim at the assessment of polysulphone calibration curves obtained under the same total ozone amount and solar zenith angle interval at different altitudes.

Acknowledgments

The authors are grateful to M G Kimlin for providing calibration curves of the USA and Australia sites. The authors thank Julian Gröbner from the Physikalisch-Meteorologisches Observatorium Davos, World Radiation Center (PMOD/WRC) for his helpful comments.

Appendix

Starting from the best fit of the polysulphone calibration curves to a polynomial function of the type

$$D = c(\Delta A + a\Delta A^2 + b\Delta A^3), \quad (\text{A.1})$$

in this work the variability of the polysulphone calibration curves is parameterized by varying the overall coefficient c and leaving the $(\Delta A + a\Delta A^2 + b\Delta A^3)$ term unchanged. This approach was suggested by Diffey (1987). Here we try to give a theoretical interpretation of equation (A.1).

The mismatch between the polysulphone action spectrum $S_{PS}(\lambda)$ and the CIE erythral action spectrum $S_{ery}(\lambda)$ causes the dependence of the polysulphone absorbance variation on the UV radiation exposure and is responsible for the variability of the polysulphone calibration curves.

The polysulphone response function at 330 nm for a monochromatic radiation of 306 nm and a polysulphone film thickness of 26 μm was studied by Krins *et al* (1999), and is given by the following expression:

$$\Delta A = -\ln \left(A + B \exp \left(-\frac{D_{\text{PS}}}{D_1} \right) + C \exp \left(-\frac{D_{\text{PS}}}{D_2} \right) \right) \quad (\text{A.2})$$

where D_{PS} is the dose weighted by the polysulphone action spectrum, D_1 and D_2 are threshold doses, A, B, C are dimensionless coefficients satisfying the condition

$$A + B + C = 1. \quad (\text{A.3})$$

The polysulphone absorbance variation is strongly dependent on the film thickness (Parisi *et al* 1999), so the coefficients given for 26 μm thickness are not valid in the case of 40 μm thickness dosimeters. Anyway, here we assume that the functional dependence of ΔA on D_{PS} is always given by equation (A.2) and that the polysulphone thickness only affects the values of the coefficients.

In order to determine A, B, C, D_1 and D_2 in the case of 40 μm thickness polysulphone films, we use the values of absorbance variations found by Diffey (1989) irradiating the dosimeters with two different calibration lamps (helarium and fluorescent lamp), whose absolute power spectra are known. Equation (A.2) can be used if D_{PS} is known. We determine D_{PS} following the definition of g given by Krins *et al* (2001), where $H(\lambda)$ is the lamp spectral irradiance:

$$g = \frac{\int S_{\text{ery}}(\lambda) H(\lambda) d\lambda}{\int S_{\text{PS}}(\lambda) H(\lambda) d\lambda} = \frac{D_{\text{ery}}}{D_{\text{PS}}}. \quad (\text{A.4})$$

By using the calibration lamps power spectra we calculate the ratio between the CIE dose, D_{ery} and the PS dose, D_{PS} . The g values obtained are $g = 0.20$ in the case of helarium lamp and $g = 0.60$ for the solar fluorescent lamp. Thus, they can be used to find the D_{PS} values helpful for best fitting to the function given by equation (A.2) leaving the five parameters free.

We find the following best fitted parameter values for the polysulphone response function in the case of 40 μm thickness:

$$\begin{aligned} A &= -0.017 \\ B &= 0.142 \\ C &= 0.875 \\ D_1 &= 2413 \text{ J m}^{-2} \\ D_2 &= 58759 \text{ J m}^{-2}. \end{aligned}$$

If we study equation (A.2) in the limit

$$\frac{D_{\text{PS}}}{D_1}, \frac{D_{\text{PS}}}{D_2} \ll 1, \quad (\text{A.5})$$

we obtain

$$\begin{aligned} \Delta A &\cong -\ln \left(A + B \left(1 - \frac{D_{\text{PS}}}{D_1} + \frac{1}{2} \frac{D_{\text{PS}}^2}{D_1^2} - \frac{1}{3!} \frac{D_{\text{PS}}^3}{D_1^3} \right) + C \left(1 - \frac{D_{\text{PS}}}{D_2} + \frac{1}{2} \frac{D_{\text{PS}}^2}{D_2^2} - \frac{1}{3!} \frac{D_{\text{PS}}^3}{D_2^3} \right) \right) \\ &= \ln \left(1 - \left(\frac{B}{D_1} + \frac{C}{D_2} \right) D_{\text{PS}} + \frac{1}{2} \left(\frac{B}{D_1^2} + \frac{C}{D_2^2} \right) D_{\text{PS}}^2 - \frac{1}{3!} \left(\frac{B}{D_1^3} + \frac{C}{D_2^3} \right) D_{\text{PS}}^3 \right). \end{aligned} \quad (\text{A.6})$$

Then, defining

$$\alpha = \frac{B}{D_1} + \frac{C}{D_2}, \quad \beta = \frac{1}{2} \left(\frac{B}{D_1^2} + \frac{C}{D_2^2} \right), \quad \gamma = \frac{1}{3!} \left(\frac{B}{D_1^3} + \frac{C}{D_2^3} \right) \quad (\text{A.7})$$

and taking into account that $\alpha \ll 1$, $\beta \sim o(\alpha^2)$, $\gamma \sim o(\alpha^3)$, we find

$$\begin{aligned}\Delta A &\cong -\ln(1 - \alpha D_{\text{PS}} + \beta D_{\text{PS}}^2 - \gamma D_{\text{PS}}^3) \\ &\cong \alpha D_{\text{PS}} - \beta D_{\text{PS}}^2 + \gamma D_{\text{PS}}^3 \\ &= \alpha D_{\text{PS}} \left(1 - \frac{\beta}{\alpha} D_{\text{PS}} + \frac{\gamma}{\alpha} D_{\text{PS}}^2\right).\end{aligned}\quad (\text{A.8})$$

Inverting this relation the following equation holds:

$$D_{\text{PS}} \cong \frac{\Delta A}{\alpha} \left(1 + \frac{\beta}{\alpha} D_{\text{PS}} - \frac{\gamma}{\alpha} D_{\text{PS}}^2 + \frac{\beta^2}{\alpha^2} D_{\text{PS}}^2 + \dots\right). \quad (\text{A.9})$$

Keeping the terms up to ΔA^3 ,

$$\begin{aligned}D_{\text{PS}} &\cong \frac{\Delta A}{\alpha} \left(1 + \frac{\beta}{\alpha} \frac{\Delta A}{\alpha} \left(1 + \frac{\beta}{\alpha} \frac{\Delta A}{\alpha}\right) + \left(\frac{\beta^2}{\alpha^2} - \frac{\gamma}{\alpha}\right) \left(\frac{\Delta A}{\alpha}\right)^2 + \dots\right) \\ &= \frac{\Delta A}{\alpha} \left(1 + \frac{\beta}{\alpha} \frac{\Delta A}{\alpha} + \left(\frac{2\beta^2}{\alpha^2} - \frac{\gamma}{\alpha}\right) \left(\frac{\Delta A}{\alpha}\right)^2 + \dots\right).\end{aligned}\quad (\text{A.10})$$

Using the definition given by equation (A.4), the relationship between the radiant exposure weighted by the CIE erythral spectrum D_{ery} and the polysulphone absorbance variation is obtained, valid in the limit of small doses:

$$D_{\text{ery}} = g \frac{\Delta A}{\alpha} \left(1 + \frac{\beta}{\alpha} \frac{\Delta A}{\alpha} + \left(\frac{2\beta^2}{\alpha^2} - \frac{\gamma}{\alpha}\right) \left(\frac{\Delta A}{\alpha}\right)^2\right). \quad (\text{A.11})$$

The calibration curve obtained is a third-order polynomial law, without the constant term, with a multiplying coefficient that is a function of the ratio g between the radiant exposure weighted by the CIE erythral curve and the radiant exposure weighted by the polysulphone spectral efficiency. All the dependence on the spectrum is in the multiplying coefficient whilst the expression in parentheses in equation (A.11) is independent of the measured spectrum, being an intrinsic characteristic of the photoinduced reaction of polysulphone film dosimeters. The g values can be estimated using equation (A.12):

$$g = 1000 \times c \times \alpha \quad (\text{A.12})$$

Values found by equation (A.12) seem to agree well with experimental data. The average of the estimated and measured g values obtained in three different field experiments performed in Rome during 2004 and 2005, where spectral UV irradiance data were available, are respectively 0.07 and 0.08.

References

- Bernhard G, Booth C R and Ehrmanjian J C 2003 Real-time UV and column ozone from multi-channel UV radiometers deployed in the National Science Foundation's UV monitoring network *Proc. SPIE, Ultraviolet Ground and Space-Based Measurements, Models and Effects III* (San Diego, Aug.) **5156** 167–78
- Boldemann C, Dal H and Wester U 2004 Swedish pre-school children's UVR exposure—a comparison between two outdoor environments *Photodermatol. Photoimmunol. Photomed.* **20** 2–8
- CIE (Commission Internationale d'Eclairage) 1987 Research note. A reference action spectrum for ultraviolet induced erythema in human skin *CIE J.* **6** 17–22
- Casale G R, Meloni D, Miano S, Siani A M, Palmieri S and Cappellani F 2000 Solar UV-B irradiance and total ozone in Italy: fluctuations and trend *J. Geophys. Res.* **105** 4895–901

- Cockell C S, Rettberg P, Horneck G, Wynn-Williams D D, Scherer K and Gugg-Helminger A 2002 Influence of ice and snow covers on the UV exposure of terrestrial microbial communities: dosimetric studies *J. Photochem. Photobiol. B* **68** 23–32
- Cockell C S, Scherer K, Horneck G, Rettberg P, Facius R, Gugg-Helminger A, Driscoll C and Lee P 2001 Exposure of arctic field scientists to ultraviolet radiation evaluated using personal dosimeters *Photochem. Photobiol.* **74** 570–8
- Davis A, Deane G H W and Diffey B L 1976 Possible dosimeter for ultraviolet radiation *Nature* **261** 169–70
- de Gruijl F R 1999 Skin cancer and solar UV radiation *Eur. J. Cancer* **35** 2003–9
- Di Menno I, Moriconi M L, Di Menno M, Casale G R and Siani A M 2002 Spectral ultraviolet measurements by a multichannel filter instrument and a Brewer spectroradiometer: a field campaign *Radiat. Prot. Dosim.* **102** 259–63
- Diffey B L 1984 Personal ultraviolet radiation dosimetry with polysulphone film badges *Photodermatol.* **1** 151–7
- Diffey B L 1987 A comparison of dosimeters used for solar ultraviolet radiometry *Photochem. Photobiol.* **46** 55–70
- Diffey B L 1989 Ultraviolet Radiation dosimetry with polysulphone film *Radiation Measurement in Photobiology* (New York: Academic) pp 135–59
- Diffey B L 2004 Climate change, ozone depletion and the impact on ultraviolet exposure of human skin *Phys. Med. Biol.* **49** R1–11
- Diffey B L and Davis A 1978 A new dosimeter for the measurement of natural ultraviolet radiation in the study of photodermatoses and drug photosensitivity *Phys. Med. Biol.* **23** 318–23
- Diffey B L and McKinlay A F 1987 A reference action spectrum for ultraviolet induced erythema in human skin *Human Exposure to Ultraviolet radiation: Risks and Regulations* ed W R Passchler and B F M Bosnjakovic (Amsterdam: Elsevier)
- Holick M F 2000 Sunlight and vitamin D: the bone and cancer connections *Radiat. Prot. Dosim.* **91** 65–71
- Kerr J B 2003 Understanding the factors that affect surface UV radiation *Proc. SPIE, Ultraviolet Ground and Space-Based Measurements, Models and Effects III* (San Diego, Aug.) **5156** 1–14
- Kimlin M G 2003 Techniques for assessing human UV exposures *Proc. SPIE, Ultraviolet Ground and Space-Based Measurements, Models and Effects III* (San Diego, Aug.) **5156** 197–206
- Kimlin M G 2005 personal communication
- Kimlin M G, Parisi A V and Wong J C F 1998a Quantification of personal solar UV exposure of outdoor workers, indoor workers and adolescents at two locations in Southeast Queensland *Photodermatol. Photoimmunol. Photomed.* **14** 7–11
- Kimlin M G, Parisi A V and Wong J C F 1998b The facial distribution of erythema ultraviolet exposure in south-east Queensland *Phys. Med. Biol.* **43** 231–40
- Kollias N, Baqer A, Sadiq I, Gillies R and Ou-Yag H 2003 Measurement of solar UVB variations by polysulphone film *Photochem. Photobiol.* **78** 220–4
- Krins A, Dörschel B, Henniger J, Knuschke P and Bais A 1999 Reading of polysulphone film after fractionated and continuous exposures to UV radiation and consequences for the calculation of the reading resulting from polychromatic UV radiation, *Radiat. Prot. Dosim.* **83** 303–7
- Krins A, Dörschel B, Knuschke P, Seidlitz H K and Thiel S 2001 Determination of the calibration factor of polysulphone film UV dosimeters for terrestrial solar radiation *Radiat. Prot. Dosim.* **95** 345–52
- Mariutti G F, Bortolin E, Polichetti A, Anav A, Casale G R, Di Menno M and Rafanelli C 2003 UV dosimetry in Antarctica (Baia Terranova): analysis of data from polysulphone films and GUV 511 radiometer *Proc. SPIE, Ultraviolet Ground- and Space-Based Measurements, Models and Effects III* (San Diego, Aug.) **5156** 254–61
- Meloni D, Casale G R, Siani A M, Palmieri S and Cappellani F 2000 Solar UV dose patterns in Italy *Photochem. Photobiol.* **71** 681–90
- Parisi A V 2005 Physics concepts of solar ultraviolet radiation by distance education *Eur. J. Phys.* **26** 313–20
- Parisi A V, Meldrum L R and Kimlin M G 1999 Polysulphone film thickness and its effects in ultraviolet radiation dosimetry. Protection Against the Hazards of UVR: Virtual Conf. 18 Jan.–5 Feb., www.photobiology.com
- Parisi A V, Wong J C F and Moore G I 1997 Assessment of the exposure to biologically effective UV radiation using a dosimetric technique to evaluate the solar spectrum *Phys. Med. Biol.* **42** 77–8
- Quintern L E, Puskeppelit M, Rainer P, Weber S, El Naggar S, Eschweiler U and Horneck G 1994 Continuous dosimetry of the biologically harmful UV-B radiation in Antarctica with the biofilm technique *J. Photochem. Photobiol. B* **22** 59–66
- Rivaton A and Gardette J L 1999 Photodegradation of polyethersulfone and polysulphone *Polym. Degradation Stab.* **66** 385–403
- Ruggaber A, Dlugi T and Nakajima T 1994 Modelling radiation quantities and photolysis frequencies in the troposphere *J. Atmos. Chem.* **18** 171–210

- El Naggar S, Hans G, Magister H and Rochlitzer R 1995 An electronic personal UV-B dosimeter *J. Photochem. Photobiol. B* **31** 83–6
- Schwander H, Koepke P and Ruggaber A 1997 Uncertainties in modelled UV irradiances due to limited accuracy and availability of input data. *J. Geophys. Res.* **102** 9419–29
- Seckmeyer G 2000 Coordinated ultraviolet radiation measurements *Radiat. Prot. Dosim.* **91** 99–103
- Siani A M, Benevento G and Casale G R 2003 Temperature dependence of Brewer UV measurements at Rome station *Proc. SPIE, Ultraviolet Ground- and Space-Based Measurements, Models and Effects III (San Diego, Aug.)* **5156** 355–66
- Sisto R, Lega D and Militello A 2001 The calibration of personal dosimeters used for evaluating exposure to solar UV in the workplace *Radiat. Prot. Dosim.* **97** 419–22
- van der Leun J C 2004 The ozone layer *Photodermatol. Photoimmunol. Photomed.* **20** 159–62
- Webb A 1995 Measuring UV radiation: a discussion of dosimeter properties, uses and limitations *J. Photochem. Photobiol. B* **31** 9–13
- Webb A 1998 *Solar UVB Instrumentation and Applications* Amsterdam (London: Gordon and Breach)
- WMO (World Meteorological Organization) 2002 *Scientific Assessment of Ozone Depletion: WMO Ozone Report* vol 47 (Geneva)